Effects of neodymium doping on the structural and magnetic properties of the double perovskite Sr2–yNdyFe1+xMo1–xO6 compound

Y Ruiz, B Aguilar, C Carvallo, J de la Torre Medina, O Navarro

I

Effects of neodymium doping on the structural and magnetic properties of the double perovskite $Sr_{2-y}Nd_yFe_{1+x}Mo_{1-x}O_6$ compound

Y. Ruiz*,†, B. Aguilar*,§, C. Carvallo‡, J. de la Torre Medina* and O. Navarro*

*Unidad Morelia del Instituto de Investigaciones en Materiales
Universidad Nacional Autónoma de México, Antigua carretera a Pátzcuaro No 8701
Col. Ex Hacienda de San José de la Huerta, 58190 Morelia, Michoacán, México

†Facultad de Ciencias Físico Matemáticas, Universidad Michoacana de San Nicolás
de Hidalgo Av. F.J. Mujica s/n Cd. Universitaria, Morelia, Michoacán, México

‡Muséum National d'Histoire Naturelle, CNRS 7590 Institut
de Minéralogie de Physique des Matériaux et des Cosmochimie,
CNRS 75005, Paris, France

§baguilar@iim.unam.mx

Received 12 August 2019
Revised 27 September 2019
Accepted 8 October 2019
Published

Curie temperature (T_C) of the ferromagnetic compound Sr_2FeMoO_6 can be modified by increasing the itinerant electrons at the Fermi level. Nd doping increases the electron density but the charge neutrality should be taken into account. In this work, a series of double perovskites $Sr_{2-y}Nd_yFe_{1+x}Mo_{1-x}O_6$ ($y = 0.0, 0.25, 0.5, 0.75$ and 1.0) for both cases, the off-stoichiometric ($x = 0$) and the stoichiometric ($x > 0$ with $x = y/2$) one, were synthesized via solid state route and discussed in detail. A crystalline structure transition was confirmed by X-ray diffraction analysis, showing a change of the lattice parameters and the unit cell volume as a function of Nd doping. It was also found that the nominal valence in Fe is mainly Fe^{3+} and in Mo is Mo^{4+}. The T_C increases continuously with Nd doping in the stoichiometric case. The increase of the T_C follows a competition with the substitution of Sr^{2+} ions by Nd^{3+} ions and the charge neutrality considered in our system.

Keywords: Double perovskite, Nd doping, Curie Temperature.

1. Introduction

The ferromagnetic oxide Sr_2FeMoO_6 (SFMO) with a double perovskite structure and strong electron correlation is considered as a fundamental compound to understand the role of electronic and magnetic properties in half-metallic systems.[1]

§Corresponding author.

SFMO has been investigated in the past decade due to attractive properties and the wide range of potential applications in spintronics[2] such as recording devices and magnetic sensors. This is attributed to the peculiar properties of SFMO, full spin polarization, low-field magnetoresistance and high Curie temperature (T_C). In the fully ordered structure of the Sr_2FeMoO_6 compound, Fe and Mo atoms occupy two interpenetrating sublattices α and β, respectively. Oxygen ions bridge the Fe and Mo atoms to form alternating FeO_6 and MoO_6 octahedra. Experimental results of the spin polarization give values of $P \approx 0.85$,[3] close to the theoretical full polarization value $P = 1$ reached for the saturation magnetization with an expected value of 4 μ_B per formula unit. One of the best experimental values for the saturation magnetization in SFMO is ≈ 3.7 μ_B,[4] discrepancy attributed to some degree of disorder between Fe and Mo atoms.[4–7]

In half-metallic materials, the challenge is to obtain higher values of T_C in order to use these materials for spintronic devices at room-temperature. Among them, the compounds Sr_2FeReO_6 and Sr_2FeMoO_6 have a fairly high T_C around 450 K,[1,8,9] the Sr_2CrReO_6 compound has a higher Curie temperature of 635 K.[10] Experimental results on SFMO have shown that a substantial increase of T_C can be observed by increasing the number of conduction electrons resulting from the substitution of divalent Sr^{2+} by trivalent La^{3+} in the Sr_2FeMoO_6 system.[11,12] Associated to this increase of T_C with the introduction of La^{3+} an important amount of disorder is induced on Fe and Mo sites, which reduce the magnetization of the SFMO system. However, recent results show that the La-doped system becomes magnetically unstable when it is over doped, giving rise to a decrease of the Curie temperature.[13]

The valence and conduction electronic bands of SFMO involve d states of the Fe and Mo transition metals with nominal configurations Fe^{3+} ($3d^5 : S = 5/2$) and Mo^{5+} ($4d^1$) with one conduction electron per Mo atom, these bands are slightly hybridized with oxygen p states lying in between Fe and Mo ions. The localized d states in Fe and Mo emphasize the strong electron correlation in SFMO, which increases the T_C.[14,15] Furthermore, half-metallicity in this compound has been described within a strong electron–electron interaction between Fe localized electrons and Mo conduction electrons,[14,16] consistent with experimental results of photoemission[17] for the ferromagnetic ground state in SFMO.

In order to have a full control of the disorder effects in SFMO, some efforts have been undertaken, studying the Fe-deficient regime and the Fe-rich composition,[5,7] the substitution of Sr with a higher cation, such as La,[11] or the doping with a smaller cation, Nd^{3+} for example Refs. 11, 18–20. Nd doping, as the case of La doping, provides an efficient way to increase the T_C but also decreases the saturation magnetization.[19] However, Nd doping could isolate the effect of electron doping in the conduction band.[21] In the following, the substitution of Sr^{2+} by Nd^{3+} in the SFMO double perovskite is analyzed experimentally taking into account the charge neutrality, we will consider the system $Sr_{2-y}Nd_yFe_{1+x}Mo_{1-x}O_6$ ($y = 0.0, 0.25, 0.5, 0.75$ and 1.0) for the stoichiometric case ($x > 0$ with $x = y/2$) and the off-stoichiometric one ($x = 0$) and discuss structural and magnetic characterization by different

techniques. However, it is important to emphasize that Nd doping induces disorder on Fe and Mo sites[11] provoking the migration of Fe atoms to Mo sites in order to balance the charge introduced by Nd into the cell.

2. Experimental Details

Polycrystalline samples of the $Sr_{2-y}Nd_yFe_{1+x}Mo_{1-x}O_6$ (SNFMO) compound with $y = 0.0, 0.25, 0.5, 0.75$ and 1.0 for the stoichiometric case ($x > 0$ with $x = y/2$) and the off-stoichiometric one ($x = 0$) were synthesized by the standard solid-state reaction method. The reactants used and provided by Sigma–Aldrich were strontium carbonate $SrCO_3$ (99.9%), neodymium oxide Nd_2O_3 (99.9%), iron oxide Fe_2O_3 (99.98%) and molybdenum oxide MoO_3 (99.99%). All the reactants were weighted according to stoichiometric amounts. The oxides and the carbonate were thoroughly mixed by mechanical milling during 4.5 h forming the first precursor phase $SrMo_{1-x}O_4$ and part of the carbonates released in the form of CO_2. In order to eliminate the remaining carbonates and to obtain the second precursor $Sr_{2-y}Nd_yFe_{1+x}O_3$, the mixed powders were calcined at 900°C during 3 h in an oven with a heating ramp of 30°C/min. In addition, powders were synthesized at 1200°C under a controlled atmosphere of 1–3% of H_2/Ar followed by a 3 h isotherm to finally obtain the double perovskite SNFMO. Structural characterization was performed by X-ray diffraction (XRD) using a Bruker X-ray diffractometer with CuKα radiation.

The oxidation states of Fe and Mo ions were studied by X-ray photoelectron spectroscopy experiments using a Physical Electronics VERSAPROBE II XPS. Moreover, the morphology of the double perovskite compounds was characterized by using a JEOL (JSM-IT300) scanning electron microscope (SEM) under high vacuum (10^{-4} Pa) conditions, the chemical homogeneity and the elemental composition of the compounds were performed by X-ray energy dispersive spectroscopy (EDS) using a 20 mm^2 Oxford X-MaxN Silicon Drift Detector (SDD) coupled to the microscope. The Curie temperature and the hysteresis loops have been obtained using a physical property measurement system (PPMS) from Quantum Design by applying the magnetic field in the range ±1.8 T.

3. Results and Discussion

The XRD patterns for the stoichiometric case are presented in Fig. 1(a) for different compositions of the double perovskite $Sr_{2-y}Nd_yFe_{1+x}Mo_{1-x}O_6$ ($y = 0.0, 0.25, 0.5, 0.75$ and 1.0) for $x > 0$ (with $x = y/2$). The ordered case SFMO ($y = 0$ and $x = 0$) is also included as a reference pattern, it shows the characteristic reflections reported early.[9] The average crystallite size of SNFMO is in the range of 30–40 nm. The patterns for $y < 0.5$ ($x = y/2$) show a displacement of the peaks to the left indicating an increase of the lattice parameters and for $y > 0.5$ ($x = y/2$) the displacement of the peaks is to the right indicating a decrease of the lattice parameters. The diffraction patterns of the stoichiometric phase for $y = 1$

($x = 1/2$) show a reflection at approximately 23° corresponding to the $NdFeO_3$ precursor phase.

In order to satisfy the charge neutrality in our Nd doping system, Fe ions tend to replace partially the sites occupied by Mo ions and the system becomes stoichiometric $Sr_{2-y}Nd_yFe_{1+x}Mo_{1-x}O_6$ for $x > 0$ (with $x = y/2$), where the number of itinerant electrons considering Fe (3+) is given by $n = 1 + y - 3x$. For $x = y/2$ ($x > 0$), the itinerant electrons decreases with Nd doping as $n = 1 - y/2$. However, it is interesting to note some important cases in our discussion; for $x = 0$ (the off-stoichiometric series $Sr_{2-y}Nd_yFeMoO_6$[18,19]), the number of itinerant electrons ($n = 1 + y$) increases with the doping, while for $y = 0$, but $x \neq 0$, the

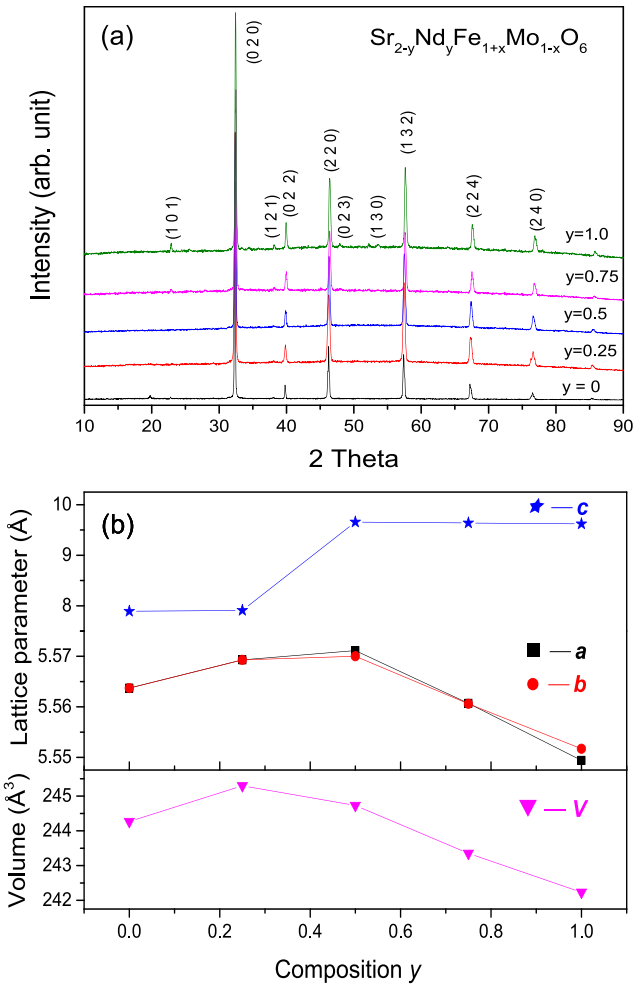

Fig. 1. (Color online) (a) XRD patterns for the double perovskite $Sr_{2-y}Nd_yFe_{1+x}Mo_{1-x}O_6$ system with $y = 0.25, 0.5, 0.75$ and 1.0 for $x > 0$ (with $x = y/2$) and (b) lattices parameters and the unit cell volume for all compositions obtained using the Rietveld method.

other stoichiometric series $Sr_2Fe_{1+x}Mo_{1-x}O_6$ is obtained,[5,7] where the number of itinerant electrons ($n = 1 - 3x$)[7] decreases for $0 < x < 1/3$ and increases for $-1 < x < 0$. By observing the limit cases of the latter system, we have that for $x = -1$ the number of itinerant electrons is $n = 2$ for $SrMoO_4$ where the valence of Mo is 4+, and for $x = 1/3$ ($n = 0$) the oxidation state of Mo is 6+, the valence of Mo cannot exceed 6+ for $x > 1/3$ and Fe cannot conserve 3+. In the limit with $x = 1$, the valence of Fe is 3+ corresponding to the $SrFeO_{3-\delta}$ and for $x = 0$ the valence is 3+ in the Sr_2FeMoO_6 compound.[5]

The crystal structure of the stoichiometric case has been characterized by the Rietveld refinement technique. The system was indexed for concentrations with $y < 0.5$ using a double perovskite crystal structure for the tetragonal space group $I4/m$ symmetry. However, for $y \geq 0.5$, it was necessary to use the monoclinic space group $P2_1/m$ to index the crystal structure, which shows a structural transition at $y = 0.5$ composition. This structural transition could be attributed to the smaller ionic size of Nd^{3+} with respect to Sr^{2+} that induces the rotation of the two-oxygen octahedral FeO_6 and MoO_6 together with the increases of the (Fe, Mo)-bond due to the electron filling. In Fig. 1(b), our refinement results show that for the tetragonal structure the lattice parameters a, b and c increase, while for the monoclinic structure, the lattice parameters a, b and c decrease. For the transition composition $y = 0.5$, even though the three lattice parameters increase, the unit cell volume decreases, see Table 1, because the structural transition involves an important change at the angle $\beta = 125.18$ between the a and c axis.

In Fig. 2, results of XPS for Fe (a) and Mo (b) in the stoichiometric double perovskite SNFMO system are presented. The spectra for $y = 0$ ($x = 0$) are included only as a reference. Figure 2(a) shows that the Fe 2p spectrum consists of Fe $2p_{3/2}$ and Fe $2p_{1/2}$ excitations at 708.4 and 721.8 eV, respectively, indicating that Fe cations are mainly Fe^{3+}, the spin-energy separations of the two excitations is 13.4 eV; it is important to note that no shift of the peaks is observed, showing that there is almost no doping effect on Fe valence and the oxidation state 3+ remaining unchanged. Figure 2(b) shows the Mo 3d spectrum consisting of two peaks from Mo $3d_{5/2}$ and Mo $3d_{3/2}$, excitations which are located at 230.9 and 234.0 eV, respectively. The intensity of these peaks increases as y increases, showing a shifting from Mo^{5+} to Mo^{4+} with Nd doping. The spin-energy separation of the

Table 1. Lattice parameters and the unit cell volume of the double perovskite $Sr_{2-y}Nd_yFe_{1+x}Mo_{1-x}O_6$ compound for $x > 0$ (with $x = y/2$).

Doping (y)	Space group	a(Å)	b(Å)	c(Å)	Vol. (Å)^3
0.0	$I4/m$	5.5637	5.5637	7.8910	244.270
0.25	$I4/m$	5.5693	5.5693	7.9083	245.300
0.50	$P2_1/m$	5.5711	5.5700	9.6563	244.730
0.75	$P2_1/m$	5.5607	5.5606	9.6386	243.353
1.0	$P2_1/m$	5.5494	5.5517	9.6202	242.232

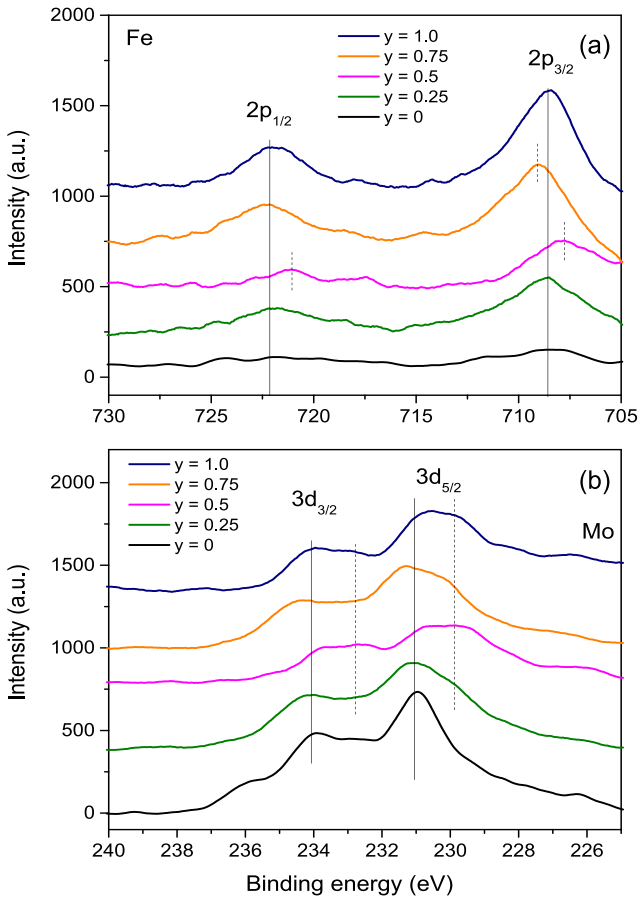

Fig. 2. (Color online) X-ray photoelectron spectra (XPS) for Fe and Mo in the double perovskite $Sr_{2-y}Nd_yFe_{1+x}Mo_{1-x}O_6$ compound for $x > 0$ (with $x = y/2$). For Fe (a) the solid lines correspond to Fe^{3+} and for Mo (b) the solid lines correspond to Mo^{5+} and the dashed lines correspond to Mo^{4+}.

two main excitations in Mo is 3.1 eV. The valence behavior of Mo is in agreement with previous results for Nd-doping.[19]

Figure 3 shows the SEM images for different compositions of $Sr_{2-y}Nd_yFe_{1+x}Mo_{1-x}O_6$ for $x > 0$ (with $x = y/2$); (a) $y = 0.0$ ($x = 0.0$) is presented only as a reference, (b) $y = 0.25$ ($x = 0.125$) and (c) $y = 1.0$ ($x = 0.5$). In this figure, it is observed that the increase of Nd content leads to larger grains whose boundaries cannot be appreciated, Nd may act as a nucleation center.[22] The EDS spectra for $Sr_{2-y}Nd_yFe_{1+x}Mo_{1-x}O_6$ are shown in Fig. 4, the EDS microanalysis has been done in different surface regions of each sample and shows the metallic content through a chemical mapping as well as an homogeneous composition of the samples. The Sr/Nd ratio changes according to the stoichiometry. The atomic percentages of each of the elements are shown in Table 2.

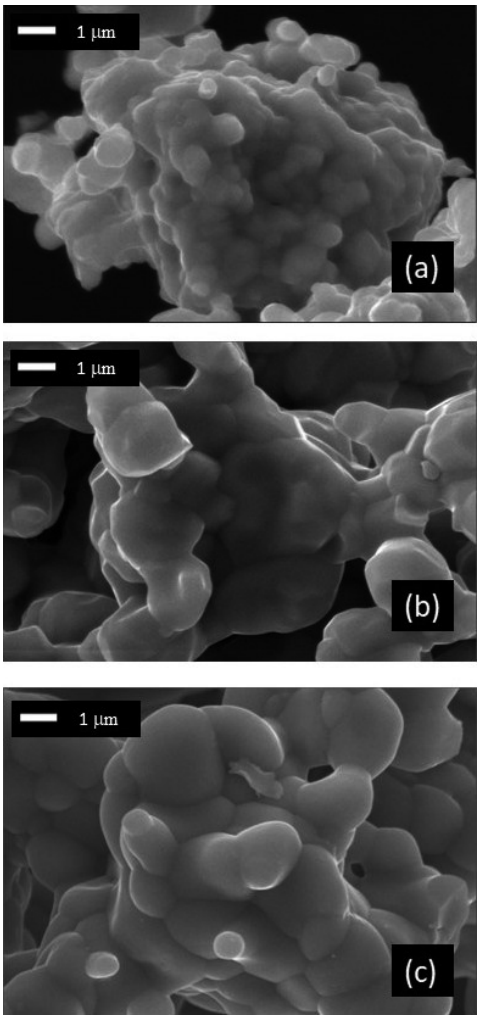

Fig. 3. SEM images for different compositions of the double perovskite $Sr_{2-y}Nd_yFe_{1+x}Mo_{1-x}O_6$ for $x > 0$ (with $x = y/2$), (a) $y = 0.0$ is the reference case, (b) $y = 0.25$ and (c) $y = 1.0$.

Susceptibility measurements of the double perovskite SNFMO compound are presented in Fig. 5. The strong influence of Nd doping can be observed in both cases for $x = 0$ (off-stoichiometry) and for $x > 0$ with $x = y/2$ (stoichiometry). For $x = 0$, the Curie temperature decreases at $y = 0.25$, which could be due to the increment of the structural distortions that prevail over the electronic effects; for high Nd doping ($y = 0.5$), the compound achieves a higher T_C in good agreement with $n = 1 + y$. It is important to note that we observe a good agreement with previous results.[21] On the other hand, for $x > 0$ ($x = y/2$), a monotonous increase of T_C is observed even for small y values, this behavior could be associated to the fact that Nd ions tend to substitute the strontium ions surrounded by iron

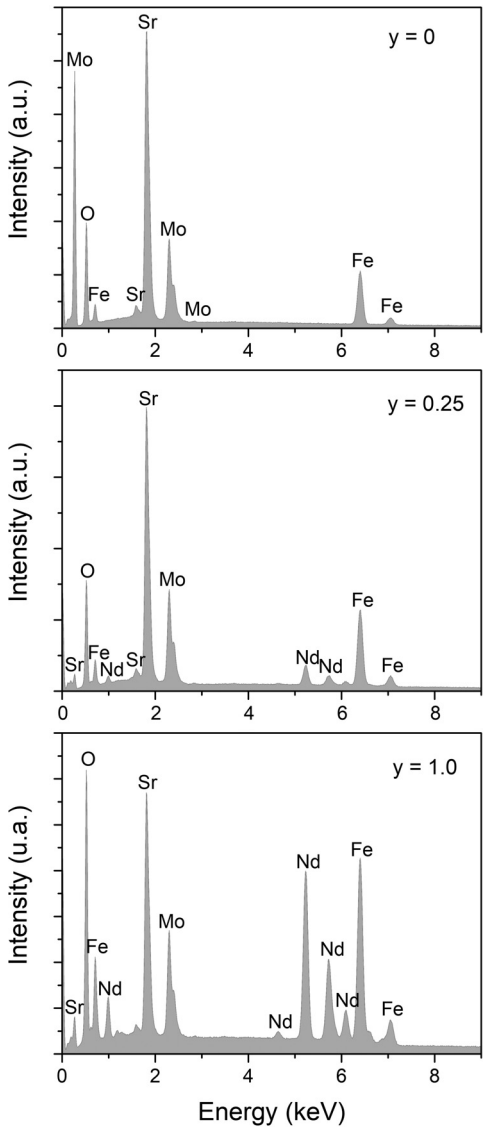

Fig. 4. EDS spectrums for different compositions of the system $Sr_{2-y}Nd_yFe_{1+x}Mo_{1-x}O_6$ ($y = 0.0$ as the reference case), $y = 0.25$ and $y = 1.0$ for $x > 0$ (with $x = y/2$).

atoms because of their oxidation states. In this case, the structural distortion is able to overcome the electronic effects. It should be noted that this behavior is valid for small concentrations of Nd doping since there is a competition with the Fe enrichment, higher values of doping ($y > 0.5$) do not show T_C.

For the magnetic characterization of the two series of $Sr_{2-y}Nd_yFe_{1+x}Mo_{1-x}O_6$ compounds with $x = 0$ and $x > 0$, hysteresis loops have been recorded by applying the external magnetic field in the range ± 1.8 T, as shown in Figs. 6(a)

Table 2. Atomic percentages for each of the elements in the $Sr_{2-y}Nd_yFe_{1+x}Mo_{1-x}O_6$ compound obtained by EDX microanalysis, $y = 0$ ($x = 0$) is included as a reference.

Element	$y = 0$	$y = 0.25$	$y = 0.5$	$y = 0.75$	$y = 1.0$
O	70.08	64.66	63.33	63.41	62.74
Fe	9.29	12.50	13.22	14.25	15.82
Sr	13.92	13.49	12.30	9.61	7.70
Mo	6.71	7.13	6.44	5.4	4.1
Nd	0	2.23	4.71	7.34	9.64

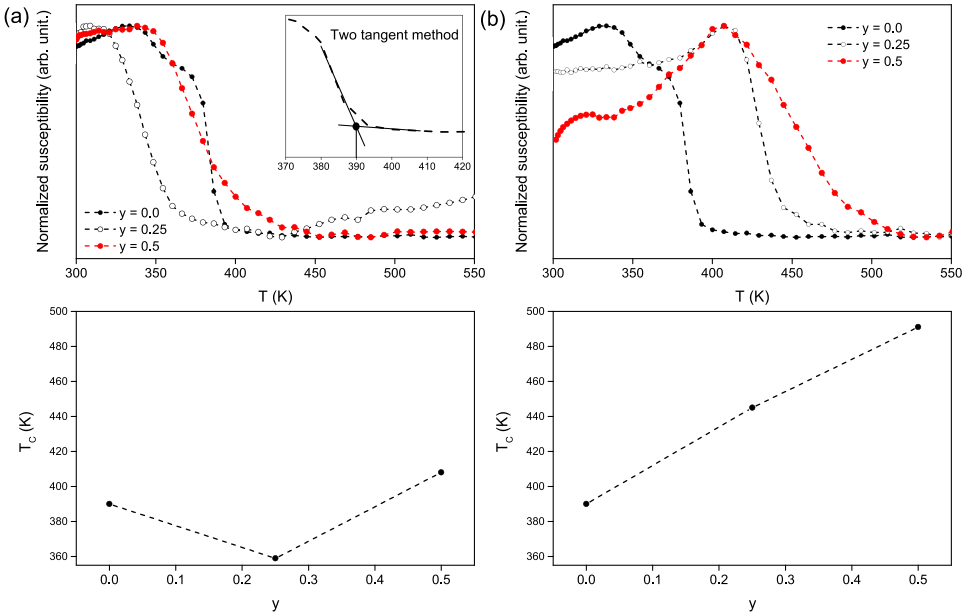

Fig. 5. (Color online) Susceptibility measurements and the Curie temperature for different compositions of the double perovskite system $Sr_{2-y}Nd_yFe_{1+x}Mo_{1-x}O_6$ ($y = 0.0, y = 0.25$ and $y = 0.5$). The off-stoichiometric case ($x = 0$) is shown in (a) and the stoichiometric case ($x > 0$, with $x = y/2$) is shown in (b).

and 6(b), respectively. The hysteresis loops for both types of compounds show a magnetization loss of about 90%, showing that replacing half of the sites occupied by Sr ions leads to an almost nonmagnetic compound. The close views of these curves at low magnetic field values (see the insets) allow to observe fine details regarding magnetic parameters like the remanence magnetization and the coercive field. Clear differences in these parameters between both series of samples arise when the lack of charge neutrality, due to the substitution of Nd in place of Sr, is overcome by balancing the Fe and Mo ions in the stoichiometric compounds $Sr_{2-y}Nd_yFe_{1+x}Mo_{1-x}O_6$. Such ionic balance has a significant impact on the magnetic behavior of the Nd-doped double perovskite, so the loss of ferromagnetism

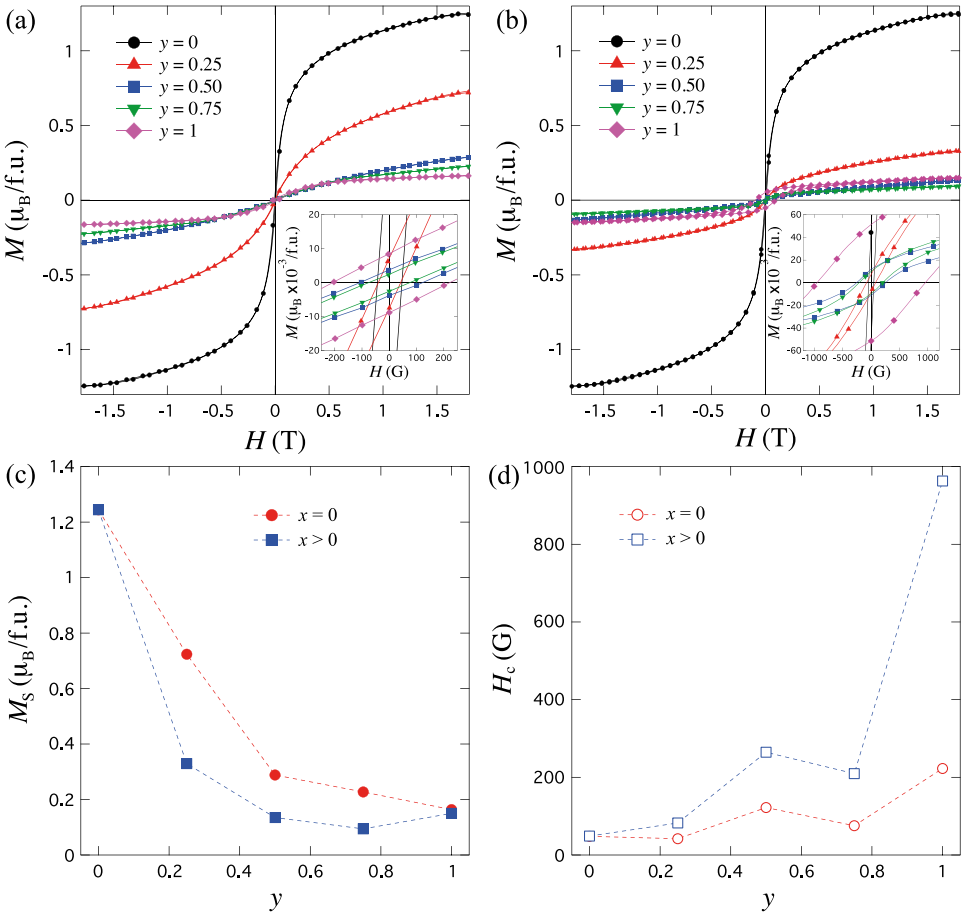

Fig. 6. (Color online) Hysteresis loops recorded in the range ±1.8 T for double perovskite compounds (a) $Sr_{2-y}Nd_yFeMoO_6$ and (b) $Sr_{2-y}Nd_yFe_{1+x}Mo_{1-x}O_6$ with different Nd contents y and for $x > 0$ (with $x = y/2$). Variation with the Nd content of (c) the saturation magnetization (M_s, at 1.8 T) and (d) the coercive field (H_c) for the double perovskite compounds of (a) and (b).

takes place faster than in the non-ion-balanced compounds, as seen in Fig. 6(c). As suggested by a previous work, the progressive reduction of M_s with y for the non-ion-balanced compounds can be ascribed to the contribution of the anti-site disorder, whereas the further reduction of M_s observed for the ion-balanced compounds can be ascribed to the electron doping.[11] In both cases, with and without charge neutrality, the coercive field increases with the Nd content because of the larger amount of domain wall pinning sites that delay the magnetization reversal process [see Fig. 6(d)]. Moreover, the increase of the coercive field for compounds with charge neutrality is consistent with a larger amount of anti-site defects that lead to antiferromagnetic regions as in the case of compounds without charge neutrality. However, the further increase for $y > 0.5$ for the former is consistent with

the structural transition observed in Fig. 1(b), which can be responsible for an additional magneto-crystalline anisotropy. Indeed, the modification of the double perovskite unit cell can influences the spin–orbit coupling that is at the origin of such kind of magnetic anisotropy, as suggested elsewhere.[23]

In conclusion, we have presented an analysis of the structural and magnetic properties of the double perovskite $Sr_{2-y}Nd_yFe_{1+x}Mo_{1-x}O_6$ system. Our results reveal a structural transition, from tetragonal to monoclinic, that occurs for the composition $y = 0.5$. The value of the maximum saturation magnetization is $\approx$1.2 μ_B/f.u. for $y = 0$, well below the optimum theoretical value 4 μ_B due to the large amount of Fe/Mo disorder in the structure. The magnetization decreases as the Nd doping increases, this is mainly caused by the antiferromagnetic interaction between the Fe–O–Fe. The XPS results for the stoichiometry compound show that as the doping increases, the Mo oxidation state shifts from 5+ to 4+ while Fe valence remains constant; this behavior could be associated to the fact that Nd ions tend to substitute the Sr ions surrounded by Fe atoms because of their oxidation states, indicating that electron injection preferentially affects the Mo cations. The Curie temperature increases for all values of Nd doping as soon as the charge neutrality is considered.

Acknowledgments

This work was partially supported by grants No. 252677 from Conacyt, PAPIIT IN105019, IN111218 and IN106619 from UNAM México. We also thank Dr. Orlando Hernández Cristóbal for preparing the SEM images, Fis. Lázaro Huerta Arcos for the XPS measurements and Prof. M. Avignon for stimulating discussion.

References

1. K. I. Kobayashi *et al.*, *Nature* **395**, 677 (1998).
2. T. K. Mandal and M. Greenblatt, in *Functional Oxides*, eds. D. W. Bruce, D. O'Hare and R. I. Walton (Wiley, 2010), pp. 257–293.
3. M. Bibes *et al.*, *Appl. Phys. Lett.* **83**, 2629 (2003).
4. Ll. Balcells *et al.*, *Appl. Phys. Lett.* **78**, 781 (2001).
5. D. Topwal *et al.*, *Phys. Rev. B* **73**, 094419 (2006).
6. B. Aguilar, O. Navarro and M. Avignon, *Microelectron. J.* **39**, 560 (2008).
7. J. R. Suárez *et al.*, *Eur. Phys. J. B* **84**, 53 (2011).
8. K. I. Kobayashi *et al.*, *Phys. Rev. B* **59**, 11159 (1999).
9. D. D. Sarma *et al.*, *Solid State Commun.* **114**, 465 (2000).
10. H. Kato *et al.*, *Appl. Phys. Lett.* **81**, 328 (2002).
11. J. Navarro *et al.*, *Phys. Rev. B* **64**, 092411 (2001).
12. B. Aguilar *et al.*, *Physica B* **556**, 108 (2019).
13. S. Jana *et al.*, *Phys. Rev. B* **86**, 29 (2012).
14. B. Aguilar, O. Navarro and M. Avignon, *Europhys. Lett.* **88**, 67003 (2009).
15. F. Estrada *et al.*, *Phys. Rev. B* **97**, 195155 (2018).
16. E. Carvajal *et al.*, *Phys. Status Solidi (B)* **242**, 1942 (2005).
17. T. Saitoh *et al.*, *Phys. Rev. B* **66**, 035112 (2002).

18. D. Rubi *et al.*, *J. Phys.: Condens. Matter* **16**, 3173 (2004).
19. A. K. Azad *et al.*, *J. Solid State Chem. B* **179**, 1303 (2006).
20. A. H. Habib *et al.*, *Physica B* **362**, 108 (2005).
21. M. Retuerto *et al.*, *Eur. J. Inorg. Chem.* 1103 (2009).
22. A. Kahoul *et al.*, *J. Appl. Phys.* **104**, 123903 (2008).
23. J. Blasco *et al.*, *Solid State Sci.* **11**, 1535 (2009).